CENTER FOR MEDICAL PHYSICS AND BIOMEDICAL ENGINEERING MEDICAL UNIVERSITY OF VIENNA

KNMF Karlsruhe NANO MICRO Facility

# Phantoms for the Quantification of spatial Resolution in multimodal Microscopy, Magnetic Resonance and Optical Coherence Tomography (OCT): first results


Andreas Berg[1,2], Antonia Lichtenegger[1], Bernhard Baumann[1], Stefan Hengsbach[3], Florian Rupp[3], Martin Börner[3], Klaus Bade[3]

[1] Center for Medical Physics and Biomedical Engineering, [2]High-Field MR-Center (MRCE); Medical University of Vienna, Austria; [3]Karlsruhe Nano Micro Facility (KNMF), Karlsruhe Institute of Technology (KIT), Eggenstein-Leopoldshafen, Germany


## 1 INTRODUCTION AND MOTIVATION

Quality control for systematic improvements in spatial resolution up to the microscopy range becomes increasingly relevant not only for preclinical imaging but also for High Field Magnetic Resonance (MR) human scanners. Phantoms for checking quantitatively and objectively the actual available spatial resolutions on an optical or MR imaging device do serve as an objective reference quality control device. Such phantoms are usually based on a set of plane grids featuring several different spatial frequencies for the quantitative evaluation of the modulation transfer function (MTF). However there are no test-structures available, that can be used for the evaluation of the MTF in 2 and 3 orthogonal dimensions for different 3D- imaging modalities in the microscopic range. We here report about the first evaluation results of a KNMF short track proposal for manufacturing these resolution phantoms using the advanced micro-structuring technologies available at the KNMF: Deep X-ray-lithography[1] and 3D-Direct laser writing[2] (Proposal-ID: 2017-018-019611): *Two- and three-dimensional Phantoms for Quantification of spatial Resolution in multimodal MR-Microscopy, µ-CT and 3D-optical Microscopic Methods (OCT).*

## 2 MATERIALS AND METHODS

### 2.1 Phantoms

Two different design concepts have been drafted for the qualitative and quantitative proof of spatial resolution for the 2-dimensional and 3D-imaging methods MR-microscopy and Optical Coherence Tomography (OCT):

#### 2.1.1 2-dimensional Test Structure Design (Phantoms)

The phantom-design is based on standard proposals for the quality control on human scanners featuring a range of grid structures with reducing periods[3,4] (fig. 1).

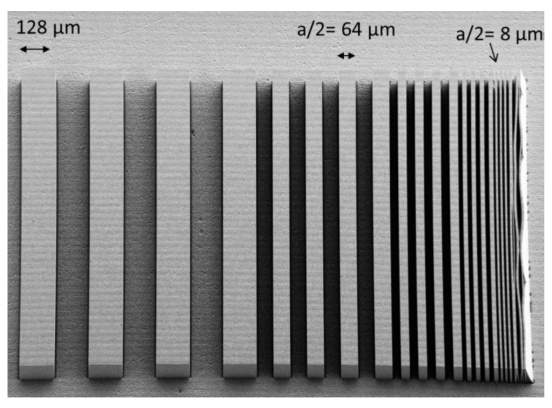


*Fig. 1 Scanning electron microscopy (SEM) image of the 2-DFT phantom. All of the grid elements feature a depth of 120 µm. The high aspect ratios (depth/width =120/8=15) could be achieved using the low divergence of Synchrotron X-rays for lithographic processing at KNMF (Deep X-ray-lithography: D-XRL).The lamellae with width ≤ 4 µm are not mechanically stable any more.*

*Funding: KNMF id: 2015-013-006488*

#### 2.1.2 3D-severe-periodic structures

The design is based on hollow cubes with polymer bars, separating cavities of different size in a 3D-arrangement. A complete set of cubes with different periodicity a is realized using 3D-Direct Laser writing 3D-DLW[1]. The web width ranges from $a_7$=4µm up to $a_2$=128µm (fig. 2).

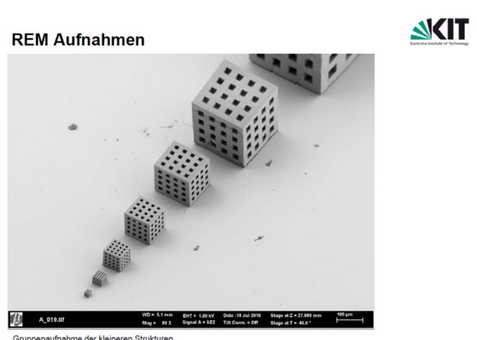


*Fig. 2 Scanning electron microscopy (SEM) image of the 3-DFT phantom.*

*Funding: KNMF iD: 2017-018-019611*

### 2.2 Imaging Methods

#### 2.2.1 MR-microscopy

MR-microscopy (MRM) is performed on a high-field (7T) human MR-scanner equipped with a prototype strong gradient system (G=750mT/m) and sensitive prototype radio-frequency detectors (rf-coils) for MR-microscopy[4] (Fig. 3b). For imaging, phase- and frequency encoding (fig. 3a) of the rf emitted signal along with slice selective excitation was used.

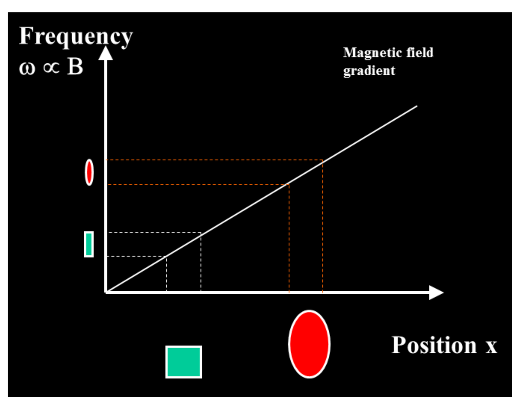


*Fig.3a Principle of frequency encoding in MR: during rf-detection a magnetic field gradient $G_x$=ΔB/Δx is applied. The precession frequency ω of the nuclear spins and subsequently the emitted rf is linearly dependent on the object position:*

$$\omega_{(x)} = \gamma\,(B_0 + G_x\, x)$$

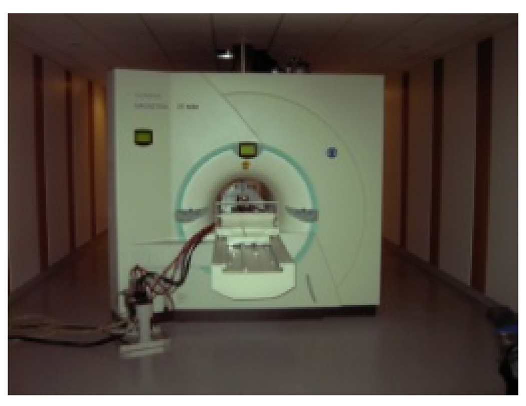

*Fig. 3b High-field (B=7T) Human-MR-Scanner with micro-imaging insert. The device for high spatial resolution in MRI relies on a strong gradient system and specially designed rf-detectors in the frame of a research cooperation and is not commercially available.*

#### 2.2.2 Optical coherence microscopy (OCM)

Optical coherence microscopy is a non-destructive optical imaging method. The image contrast is based on the intrinsic scattering of light within the tissue using the low-coherence interferometric light backscattered from the investigated tissue with a reference light beam. High-resolution, two- and three-dimensional images can be created in real time (fig. 4).

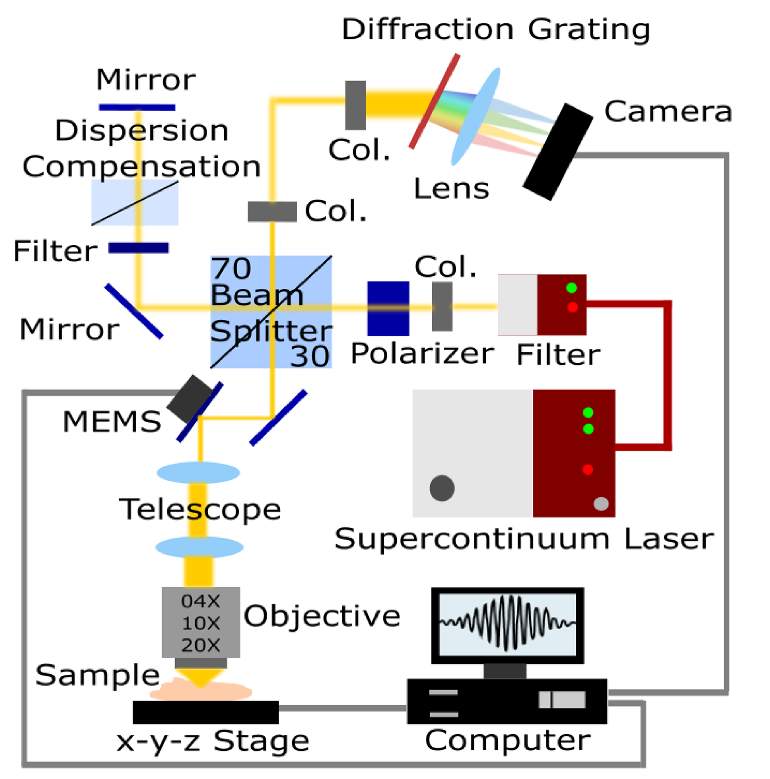


Funding: European Research Council (ERC StG 640396 OPTIMALZ)

*Fig. 4 Sketch of the visible light OCM system [5]. Utilizing a broad-band supercontinuum laser a nominal resolution (spatial coherent length) of 1 µm in depth (1.2 µm in air) was achieved. The lateral resolution is mainly limited by the aperture of the objective. The OCM prototype system was used for preclinical and ex-vivo tissue investigations (MEMS: Microelectromechanical Mirror, Col.: Collimator).*

## 3 RESULTS

### 3.1 2-dimensional MR-microscopy

The slice-selective encoding was adjusted to the layer of the 2D-grid phantom such, that both of the orthogonal grids could be observed (fig. 5). Visual qualitative inspection in vertical direction indicates, that the grid period of $a_3$=64µm (lamellae-width $a_3/2$=32µm) could be differentiated. However the same grid in horizontal direction is hardly to be visualized at pixel-size of 31µm.

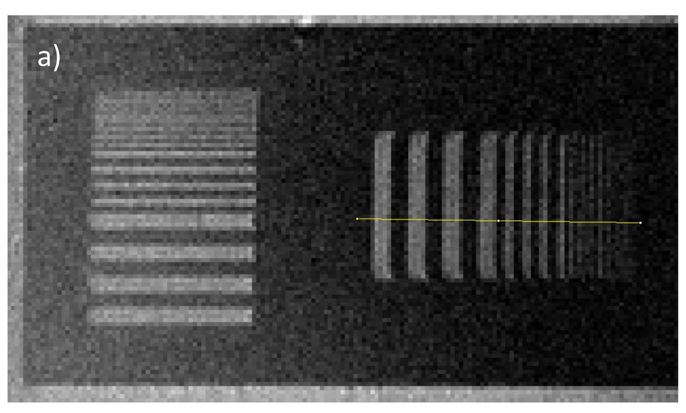


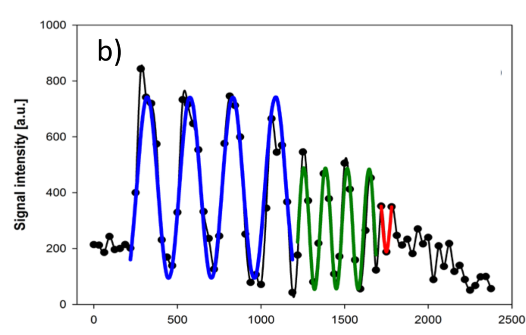


*Fig. 5b (top right) Intensity profile for evaluation of the relative modulation depth and the MTF.*

*Fig. 5a Realistic example of a slice selective MR-scan (Vs: 31x31x120µm³. Mtx:160x320, 3 sl, TA<5min) of the phantom positioned in the plane of the 2 orthogobe visualizednal grids. (yellow line: profile path for determination of the MTF (fig.5b). The resolution criterion ($M_{r(Kres)}$=0,5!) delivers a critical spatial frequency:$K_{res}$≈10.4 lp/mm, which corresponds to a smallest detectable structure (spatial resolution): a/2≈48µm>>31µm (pixel size).*

### 3.2 3-dimensional MR-microscopy

A multi-slice 3D Turbo-spin echo sequence (TE=17ms TR=3s, av: 8) allowed for obtaining isotropic voxel sizes and visualization of the largest cubes (fig.6).

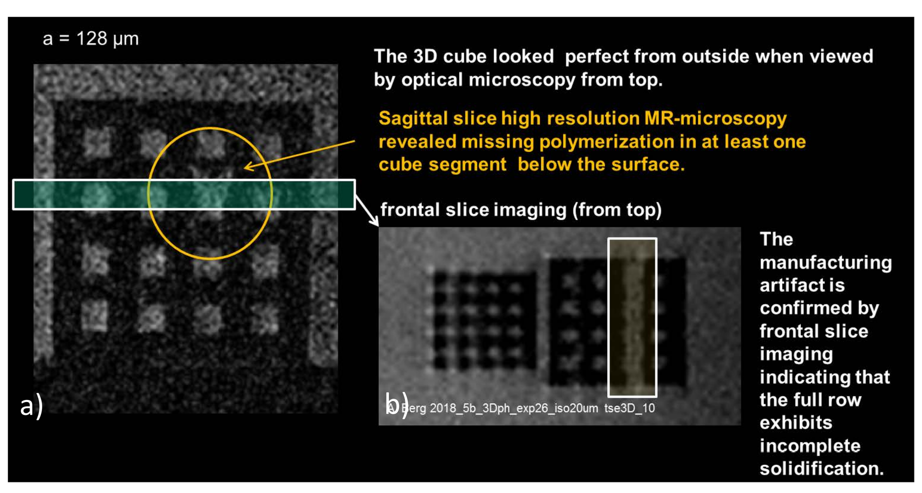


*Fig. 6a (left) 3D-multi-slice MR-microscopy: lateral 2D-view of the cube $a_2/2$ = 64 µm. A manufacturing artefact in 2nd row inside the cube is discovered, which extends for the whole orthogonal row as seen in the en-face view **(b) right bottom)** of the corresponding slice, visualized from the same 3D-MRI data set. Such type of manufacturing errors inside the object can hardly be detected by surface scanning techniques as scanning electron microscopy SEM (cf. fig. 2) and standard optical microscopy (see fig. 7).*

### 3.2 Standard 2D- optical Microscopy and 3-dimensional Optical Coherence Microscopy (OCM)

3.2.1 Standard optical microscopy resolved the surface structure of all of the 3D cubes. However the manufacturing artefact inside the largest cube could not be visualized (fig. 7).

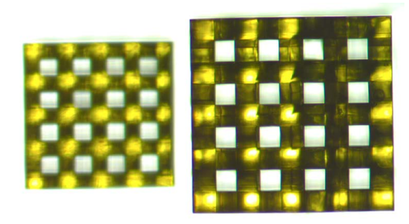

*Fig.7 Standard optical microsope images for the largest cubes ($a_2$=128µm and $a_{2b}$=92µm). Note that the missing line in 2nd row inside the cube below the top layer cannot be visualized directly.*

3.2.2 OCM acquires volumetric data sets, allowing the visualization in selected slices. En-face images (views from top in fig. 2) are shown in fig. 8a. Even the smallest cube with a=4 um can be resolved in these en-face images.

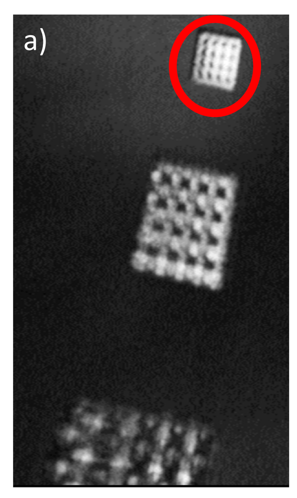


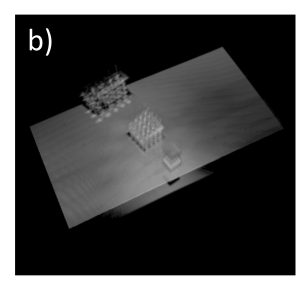


***Fig.8b** OCM 3D-renderings of 3D-DLW cubes $a_7$ = 4 µm (right, bottom), $a_6$ = 8 µm (medium) and $a_5$ = 16µm (left,top).*

***Fig.8a (left)** Optical coherence microscopy (OCM) en-face view (from top; averaged ≥1 µm thick slices). Note the contrast between the hollow areas and the polymer resist bars of the 3D-grid featuring a lateral size $a_7/2$= 2µm (top).*

## 4 SUMMARY AND CONCLUSION

An orthogonal set of grids featuring periodic bar-slit couples between $a_1/2$ = 128 µm and $a_5/2$ = 8 µm at structural depth of 120 µm was manufactured using deep X-ray lithography with excellent straight walls and congruent bar-to-slit width. We were not successful in manufacturing smaller structures than 8 µm as defined by the design and mask, mainly due to mechanical instabilities of the thin lamellae. The structure can conveniently be used for a qualitative quick check on spatial resolution in MRM for 99% of actual MRM scanner devices. Moreover the Modulation Transfer Function (MTF) in two orthogonal directions e.g. for phase and frequency encoding can be easily derived from a profile measurement. The quantitative determination of spatial resolution can be obtained using a resolution criterion based on the minimum relative modulation depth or modulation-to-noise ratio. Using 3D-Direct-Laser writing (3D-DLW), we were able to manufacture a complete set of 3D-cubes with bar width between $a_2$=128 µm and $a_7$=4 µm. This new design and prototype cube set can be used for checking spatial resolution in-plane including impact of different slice thickness for 3D-MR-microscopy and optical coherence microscopy (3D-resolution).

## 5 REFERENCES


[1] Saile V, (ed.), Wallrabe U, (ed.), Tabata O (ed.), Korvink JG (ed.); *LIGA and Its Applications*; in: Advanced Micro & Nanosystems 7, 1; Wiley-VCH (2009) ISBN 978-3-527-31698-4.
[2] Hengsbach S, Diaz Lantada A; *Rapid prototyping of multi-scale biomedical microdevices by combining additive manufacturing technologies*; Biomed Microdevices, DOI 10.1007/s10544-014-9864-2.
[3] Berg A, *Testphantom zur Kontrolle der Abbildungsqualität in der hochortsauflösenden NMR-Bildgebung* Deutsches Patentamt, München(IPC): G01R 33/58, G01N24/08; DE19904635; 1999-08-19.
[4] Berg A, Potthast A, Starewicz P; *MR-MICROSCOPY ON A HUMAN 7T-SCANNER;* Proc. ISMRM/ESMRMB 2010, progr nr. 1048; Stockholm, Sweden , 01.-07.05.2010 (2010).
[5] Lichtenegger A et al; *Spectroscopic imaging with spectral domain visible light optical coherence microscopy in Alzheimer's disease brain samples;* Biomed. Opt. Express **8**, 4007-4025 (2017).